

Eliminating the zero spectrum in Fourier transform profilometry using a two-dimensional continuous wavelet transform

Munther A. Gdeisat ^{*}, David R. Burton, Michael J. Lalor

General Engineering Research Group (GERI), Liverpool John Moores University, James Parsons Building Room 114, Byrom Street, Liverpool L3 3AF, United Kingdom

Received 3 March 2006; received in revised form 9 May 2006; accepted 16 May 2006

Abstract

In this paper, a filtering technique based upon two-dimensional continuous wavelet transform (2D-CWT) is used to eliminate the low frequency components of fringe patterns. The filtered fringe patterns are subsequently demodulated using a standard Fourier transform profilometry (FTP) algorithm. This image pre-filtering stage improves the noise performance of the FTP algorithm and enables the FTP method to demodulate fringe patterns with larger bandwidths. Also, the 2D-CWT technique reduces speckle noise significantly. Moreover, only a single fringe pattern is required in this technique. The 2D-CWT algorithm is capable of separating low frequency terms from the high frequency terms that contain phase-modulated fringe information, even when both interfere, greatly, in the frequency domain. The proposed algorithm is tested, both via computer simulation and using real fringe patterns. This revealed the robustness of this algorithm and also demonstrably enables the demodulation of a wider range of fringe patterns using the FTP technique.

© 2006 Elsevier B.V. All rights reserved.

PACS: 07.05.Pj; 42.30.Rx; 42.30.Ms

Keywords: Image processing; Phase retrieval; Speckles

1. Introduction

Recently, there has been much interest in demodulation of fringe patterns using digital computers. This has many medical and industrial applications [1,2]. There are many methods that can be used to demodulate fringe patterns such as Fourier transform profilometry (FTP) [3], phase stepping [4], digital phase locked loop [5], and direct phase detection [6]. Probably the most commonly used of these techniques are the first two.

A common procedure used as part of the FTP algorithm involves removing low frequency components of a fringe

pattern, which represent background illumination in the image. This step is easy to perform if the low frequency components are separated in the frequency domain from the high frequency components that contain the phase-modulated fringe information. In this case, filtering in the frequency domain is carried out to remove the low frequency spectrum [3,7].

The spectrum of the low frequency components may interfere with the spectrum of the high frequency components. Consequently, it is not possible to separate them using filtering techniques in the frequency domain. This crosstalk distortion occurs due to reasons related to the Fourier transform algorithm itself such as the leakage phenomena [8].

A common reason for crosstalk distortion between the zero peak and the fringe information is a large variation

^{*} Corresponding author. Tel.: +44 151 231 2365; fax: +44 151 298 2447.
E-mail addresses: m.a.gdeisat@ljmu.ac.uk (M.A. Gdeisat), d.r.burton@ljmu.ac.uk (D.R. Burton), m.j.lalor@ljmu.ac.uk (M.J. Lalor).

in surface slope on the surface to be measured. This variation leads to the fringe pattern having a higher modulation index and thus a relatively large bandwidth. Frequency content within the fringe pattern may then vary from very high on one side of a slope to very low on the reverse side. It is this very low element that can interfere and merge with the zero order peak. Attempts to remove this by rearranging the illumination direction are not always possible and the use of frequency plane filtering within the Fourier transform fringe analysis method simply results in us losing surface information in the low fringe frequency regions [9].

For complex objects, while the removal of the low frequency spectrum is very difficult to achieve in the frequency domain, many algorithms have been proposed to alternatively remove it in the spatial domain. Jian et al. have used a sinusoidal grating projection and a π phase shifting technique to eliminate the background illumination of the fringe pattern [10].

Lilley et al. have suggested another method to remove the background illumination of a fringe pattern generated by a twin-fiber interferometer [1]. In this method, a fringe pattern is captured, and then one of the fibers is vibrated at 500 Hz. A second image is captured during the vibration of one of the fibers. The second image can be considered as the background illumination of the fringe pattern. During the vibration of one of the fibers, the camera sees the average intensity of the fringes. The background illumination image is subtracted from the fringe pattern and the mathematical mean of the resultant image is close to zero.

Both techniques in [1,11] require the capture of another image in order to remove the background illumination term from the fringe pattern. This limits the use of the FTP method to the measurement of fairly static objects.

Chen et al. have proposed the use of the windowed Fourier transform (Gabor transform) to eliminate the zero spectrum in fringe patterns [11]. In this method, the zero component of the deformed fringe pattern is extracted using the windowed Fourier transform. The normalized Fourier spectrum for the deformed fringe pattern is calculated. Finally, the zero component is subtracted from the spectrum of the deformed fringe pattern. The resultant spectrum is then used by the FTP technique. As will be demonstrated in this paper, Chen's technique is not capable of eliminating the zero spectrum in fringe patterns that have large bandwidths. Also, in the cases where the existence of large levels of speckle noise corrupts the fringe patterns, this algorithm may not be capable of extracting the low frequency components.

In this paper, we present a new technique for the elimination the low frequency components of fringe patterns using a two-dimensional continuous wavelet transform (2D-CWT) filtering technique [12]. The filtered fringe pattern is then demodulated using a standard FTP technique. The proposed technique outperforms Chen's algorithm. It

is capable of removing the background illumination of fringe patterns that have large bandwidths. Also, it considerably reduces speckle noise. Moreover, it is capable of removing the background illumination of fringe patterns that are corrupted with high levels of speckle noise.

In Section 2, we present the background theory of the FTP algorithm. Section 3 introduces the 2D-CWT algorithm and discusses the use of this algorithm to remove the background illumination of fringe patterns. In Section 4, computer simulation is used to test the validity of the proposed algorithm and compare its performance with Chen's algorithm. In Section 5 results from the application of the proposed technique to background illumination removal in real fringe patterns are presented and discussed. Also, the performance of the proposed technique is compared with Chen's algorithm using real fringe patterns.

2. Fourier fringe analysis

The intensity of a fringe pattern can be expressed as:

$$g(x, y) = \alpha(x, y) + \beta(x, y) \cos(2\pi f_0 x + \phi(x, y)) \quad (1)$$

where $\alpha(x, y)$ represents the background illumination, $\beta(x, y)$ the amplitude modulation of the fringes, f_0 the spatial carrier frequency, $\phi(x, y)$ the phase modulation of fringes and x and y the sample indices for the x and y axes, respectively. For simplicity, it is considered here that there is no carrier frequency on the y -axis (i.e., the projected fringes lie parallel to the y -axis). The previous equation can be rewritten as [13]:

$$g(x, y) = \alpha(x, y) + c(x, y) \exp(j2\pi f_0 x) + c^*(x, y) \exp(-j2\pi f_0 x) \quad (2)$$

where $c(x, y) = \frac{\beta(x, y) \exp(j\phi(x, y))}{2}$ and $c^*(x, y)$ represents the complex conjugate of $c(x, y)$. The two-dimensional discrete Fourier transform (2D-DFT) is performed for the fringe pattern and the spectrum of the fringe pattern can be expressed as:

$$G(f_x, f_y) = A(f_x, f_y) + C(f_x - f_0, f_y) + C^*(f_x + f_0, f_y) \quad (3)$$

where $A(f_x, f_y)$ describes the low frequency spectrum of the background illumination, $C(f_x - f_0, f_y)$ and $C^*(f_x + f_0, f_y)$ are the spectra of the deformed fringes. In some cases, the spectrum of the background illumination is separated from the spectrum of the deformed fringes; consequently, the background illumination can be filtered out. The spectrum of the modulated fringes is separated into two symmetrical components, and either one of them contains the desired phase information, which is proportional to the height of the object. One of the components, let us say $C(f_x - f_0, f_y)$, is separated by a window and the filtered spectrum is transformed back to the spatial domain by the application of the two-dimensional inverse discrete Fourier transform (2D-IDFT). The real components of the inverse Fourier transform are the filtered fringe pattern,

whereas the imaginary components of the inverse Fourier transform are a $\pi/2$ phase shifted version of the filtered fringe pattern. The real components can be expressed as:

$$\Re\{c(x, y)\} = \beta(x, y) \cos(2\pi f_0 x + \phi(x, y)) \quad (4)$$

The imaginary components can be described as

$$\Im\{c(x, y)\} = \beta(x, y) \sin(2\pi f_0 x + \phi(x, y)) \quad (5)$$

The desired phase information can be extracted point-wise through the equation:

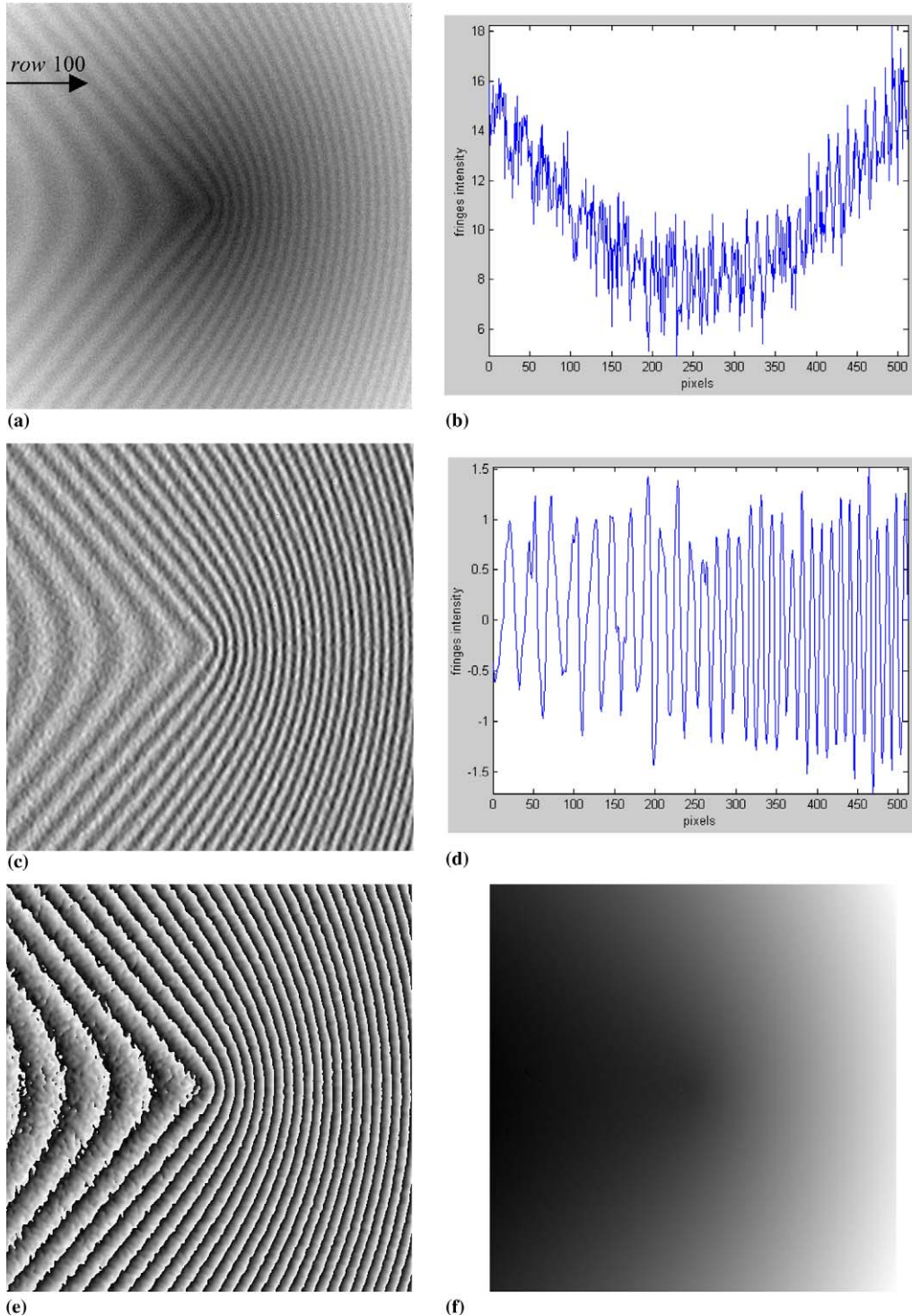


Fig. 1. (a) A computer-generated fringe pattern, (b) row 100 of the fringe pattern, (c) the filtered fringe pattern using the 2D-CWT proposed algorithm, (d) row 100 of the filtered fringe pattern, (e) and (f) the wrapped and unwrapped phase maps produced by the application of FTP to the fringe pattern shown in (c).

$$\begin{aligned}
\varphi(x, y) &= \tan^{-1} \frac{\Im\{c(x, y)\}}{\Re\{c(x, y)\}} \\
&= \tan^{-1} \left(\frac{\beta(x, y) \sin(2\pi f_0 x + \phi(x, y))}{\beta(x, y) \cos(2\pi f_0 x + \phi(x, y))} \right) \\
&= \tan^{-1} \{\tan(2\pi f_0 x + \phi(x, y))\} \\
&= [2\pi f_0 x + \phi(x, y)] \bmod \pi
\end{aligned} \tag{6}$$

where mod represents the modulo function (i.e. $r \bmod \pi$ expresses the remainder when r is divided by π). The resultant phase is limited between $-\pi$ and π due to the application of the arctangent function. The resultant phase should be unwrapped in order to remove the 2π steps. The unwrapped phase contains the desired phase information and the spatial carrier frequency, which should be removed.

The Fourier fringe analysis algorithm suffers from some problems in the frequency domain filtering such as leakage and crosstalk. The Fourier transform assumes that the signal is infinite in the time domain. The discrete Fourier transform takes part of the infinite signal and assumes that it is periodic, and this process is called truncation. The truncated signal should be an integer number of periods of the signal; otherwise, high frequency components are produced

[8]. During the filtering in the frequency domain, the inclusion of these high frequency components will include the high frequency noise in the filtered fringe pattern. Conversely, the exclusion of the high frequency components will introduce errors at the borders of the demodulated phase map. This problem can be alleviated by multiplying the fringe pattern by a window such as the Hamming window [13]. Crosstalk happens due to the interference between the spectrum of the background illumination in the fringe pattern and the spectrum of the modulated fringes.

3. Application of 2D-CWT in FTP

In the one-dimensional continuous wavelet transform, a signal $f(x)$ is projected onto the wavelet $\psi_{b,s}$ by translation on the x -axis by b and dilation by s of the mother wavelet $\psi(x)$. The resulting wavelet transform is two-dimensional. In the 2D-CWT, the image $f(x, y)$ is projected onto the wavelet $\psi_{a,b,s,\theta}$ by translation on x and y axes by a and b , respectively, dilation by s , and rotation by the angle θ of the mother wavelet $\psi(x, y)$. The resulting wavelet transform is four-dimensional [12,14]. The wavelet transform of an image $f(x, y)$ is given by:

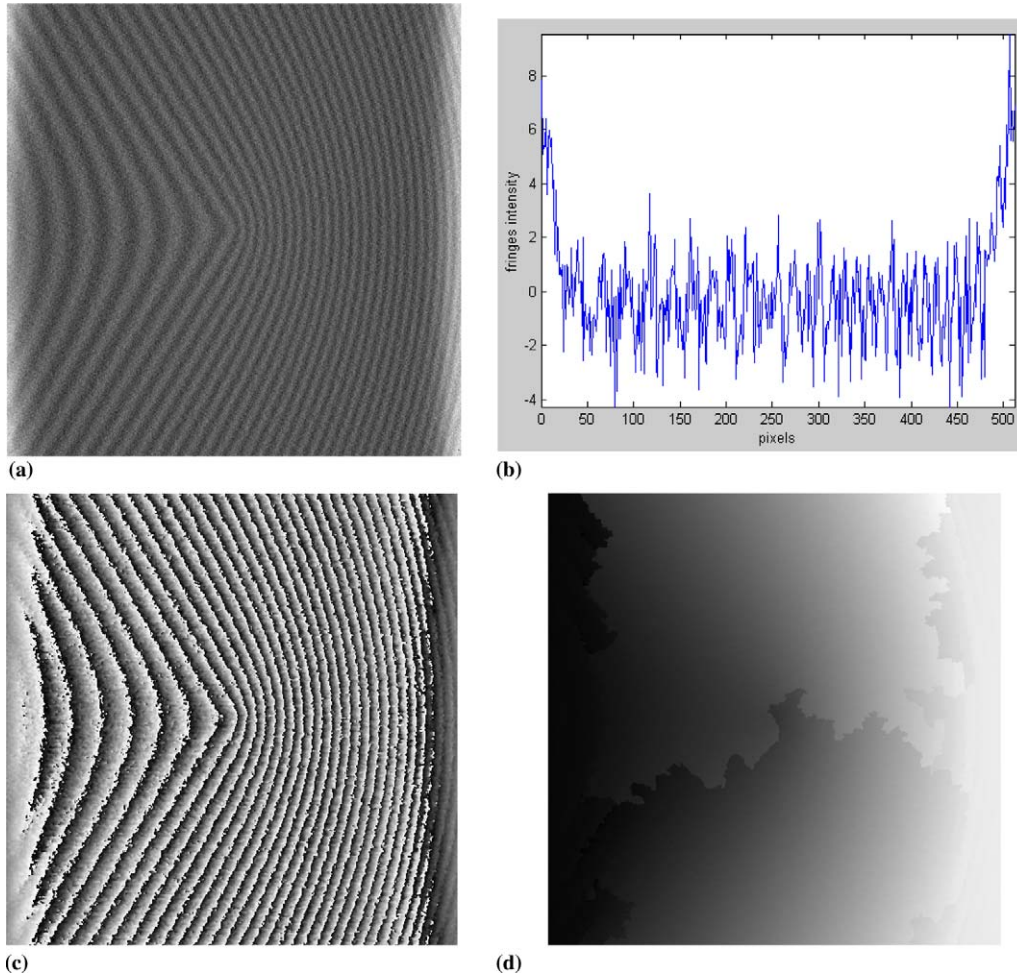


Fig. 2. (a) Resultant image of applying Chen's algorithm to a computer-generated fringe pattern, (b) row 100 of the filtered fringe pattern, (c) and (d) the wrapped and unwrapped phase maps produced by the application of FTP to the fringe pattern shown in (a).

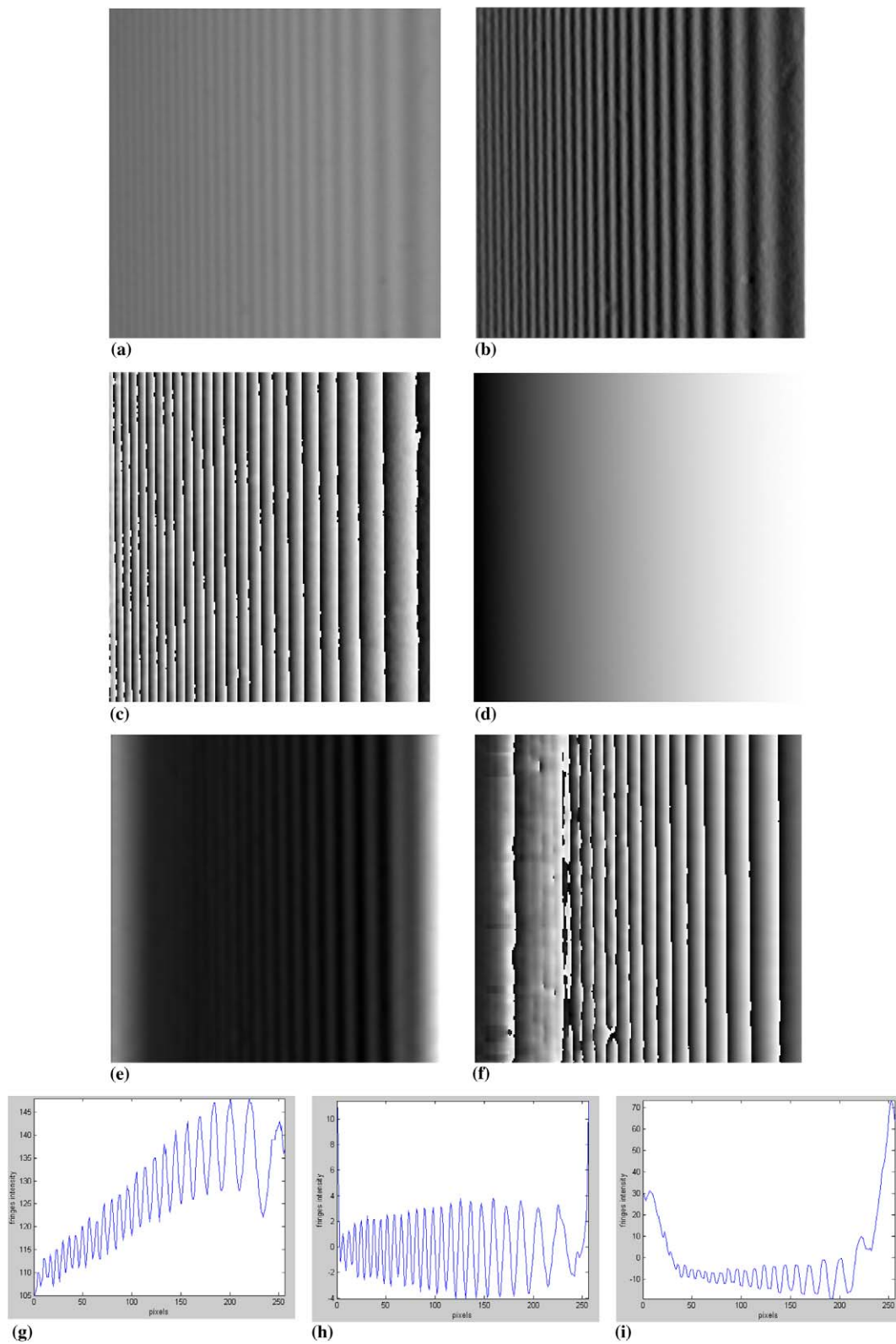


Fig. 3. (a) A real fringe pattern is filtered using the 2D-CWT method (b) and Chen's algorithm (c). The filtered image in (b) is processed using the FTP technique and the resultant wrapped and unwrapped phase maps are in (d) and (e), respectively. (f) The wrapped phase map produced by processing the image in (e) using the FTP technique. (g)–(i) row 100 of the fringe patterns shown in (a), (b) and (e), respectively.

$$S(a, b, s, \theta) = \langle \psi_{a,b,s,\theta}, f(x, y) \rangle$$

$$= s^{-1} \iint \psi\left(\frac{x-a}{s}, \frac{y-b}{s}, r_\theta\right) f(x, y) dx dy \quad (7)$$

The mother wavelet $\psi(x, y)$ must satisfy the admissibility condition:

$$c_\psi \equiv (2\pi)^2 \iint \frac{\hat{\psi}(f_x, f_y)}{f_x^2 + f_y^2} ds dr < \infty \quad (8)$$

where $\hat{\psi}(f_x, f_y)$ is the Fourier transform of $\psi(x, y)$.

The two-dimensional mother wavelets can be classified into two groups: isotropic and directional wavelets. In fringe pattern applications, the isotropic wavelets are used for filtering purposes, whereas the directional wavelets are used for phase demodulation of fringes [15]. The mother wavelet used in this paper belongs to the isotropic group.

In this paper, we propose the use of the two-dimensional first derivative of Gaussian (DoG) wavelet to filter out the background illumination in fringe patterns [16]. The first derivative of Gaussian wavelet is given by:

$$\psi(x, y) = \sqrt{x^2 + y^2} \exp\left(-\frac{1}{2}(x^2 + y^2)\right) \quad (9)$$

with the Fourier transform

$$\hat{\psi}(f_x, f_y) = -i\sqrt{f_x^2 + f_y^2} \exp\left(-\frac{1}{2}(f_x^2 + f_y^2)\right) \quad (10)$$

The DoG 2D-CWT is used here to extract the deformed fringes and filter out the background illumination. The filtered fringes are then applied to the FTP algorithm to extract the phase of the fringe pattern.

4. Computer simulation

In the numerical simulation, a simulated 3D object was used to phase-modulate a computer-generated fringe pattern. The resultant deformed fringe pattern is an image of size 512×512 pixels and used to test the proposed algorithm. The object is given by

$$\phi(x, y) = 0.2((x - 256)^2 + (y - 256)^2)^{1/2} \quad (11)$$

and the fringe pattern is given by

$$I(x, y) = 0.25\phi(x, y) + \cos(2\pi f_0 x + \phi(x, y)) + \text{noise} \quad (12)$$

The noise is uniformly distributed and its variance was set to 1.2. The spatial frequency f_0 was set to 1/16. The computer-generated fringe pattern is shown in Fig. 1(a). Row 100 is shown in Fig. 1(b).

The fringe pattern was processed and filtered using the 2D-CWT algorithm with scale 2 and angle 0. The resultant fringe pattern is shown in Fig. 1(c). Row 100 of the filtered fringe pattern is shown in Fig. 1(d). The filtered fringe pattern was then demodulated using the FTP algorithm. The resultant wrapped phase map is shown in Fig. 1(e). The wrapped phase map was unwrapped using the phase unwrapping algorithm in [17] and the unwrapped phase map is shown in Fig. 1(f) in gray scale. The white color indicates large values, whereas the black color indicates small values.

Increasing the value of the scale improves the ability of the 2D-CWT algorithm in removing speckle noise and reduces its capability of filtering out the background illumination of the fringe pattern. Conversely, setting the scale to a small value reduces the ability of the algorithm in removing the speckle noise and enhances its performance in removing the background illumination of a fringe pattern even if its spectrum is highly interfered in the frequency domain with the spectrum of modulated fringes.

In the case of fringe patterns that are highly corrupted with speckle noise and the spectrum of its background illumination interferes largely with the spectrum of modulated fringes, the filtering process may be carried out in two stages. Initially the speckle noise is removed by processing the fringe pattern using large-scale values, for example larger than 2. Then the resultant image is processed using small-scale values (e.g., less than 1).

The value of the angle depends on the direction of fringes and should be set to zero if the direction of fringes is parallel to the y -axis. On the other hand, when the direction of fringes is parallel to the x -axis, then the angle value shown be set to $\pi/2$.

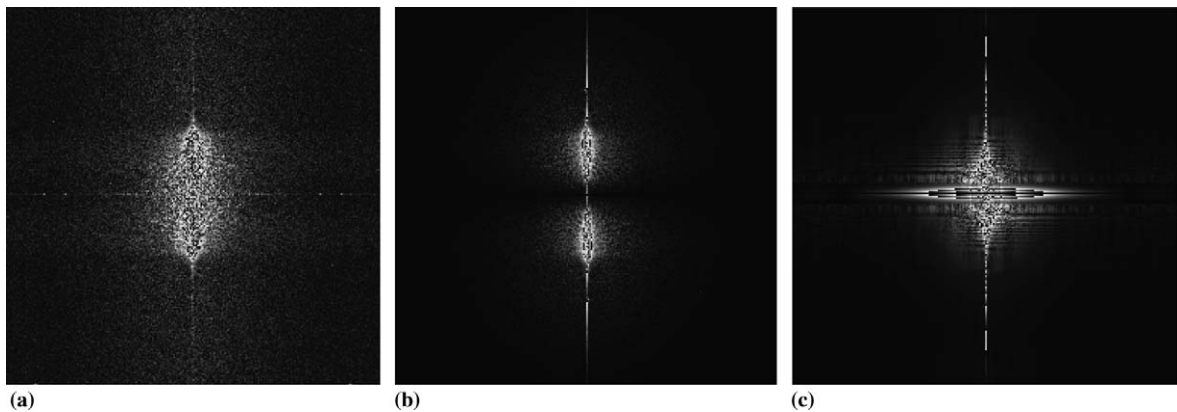


Fig. 4. (a)–(c) The spectrum of the fringe patterns shown in Figs. 3(a), (b) and (e), respectively.

For the purpose of comparison, the fringe pattern shown in Fig. 1(a) has also been processed using Chen's algorithm in order to remove the background illumination and the results are shown in Fig. 2(a). Row 100 of the filtered fringe pattern is depicted in Fig. 2(b). The distortion at the left and right borders of the fringe pattern can be clearly observed. The filtered fringe pattern was applied to the FTP algorithm and the resultant wrapped phase map is shown in Fig. 2(c). The phase map was unwrapped using the algorithm in [18] and the resultant image is shown

in Fig. 2(d). The window width and the moving factors were to 64 and 3, respectively [11].

The window width in Chen's algorithm should be set to a small value (e.g., 16, 32) to process fringe patterns with narrow bandwidths. This reduces the distortion at the borders of the fringe pattern. Conversely, when processing fringe patterns with wide bandwidths, the window width should be set to a large value such as 64. This may introduce distortions at the edges of the fringe pattern that the FTP algorithm cannot tolerate.

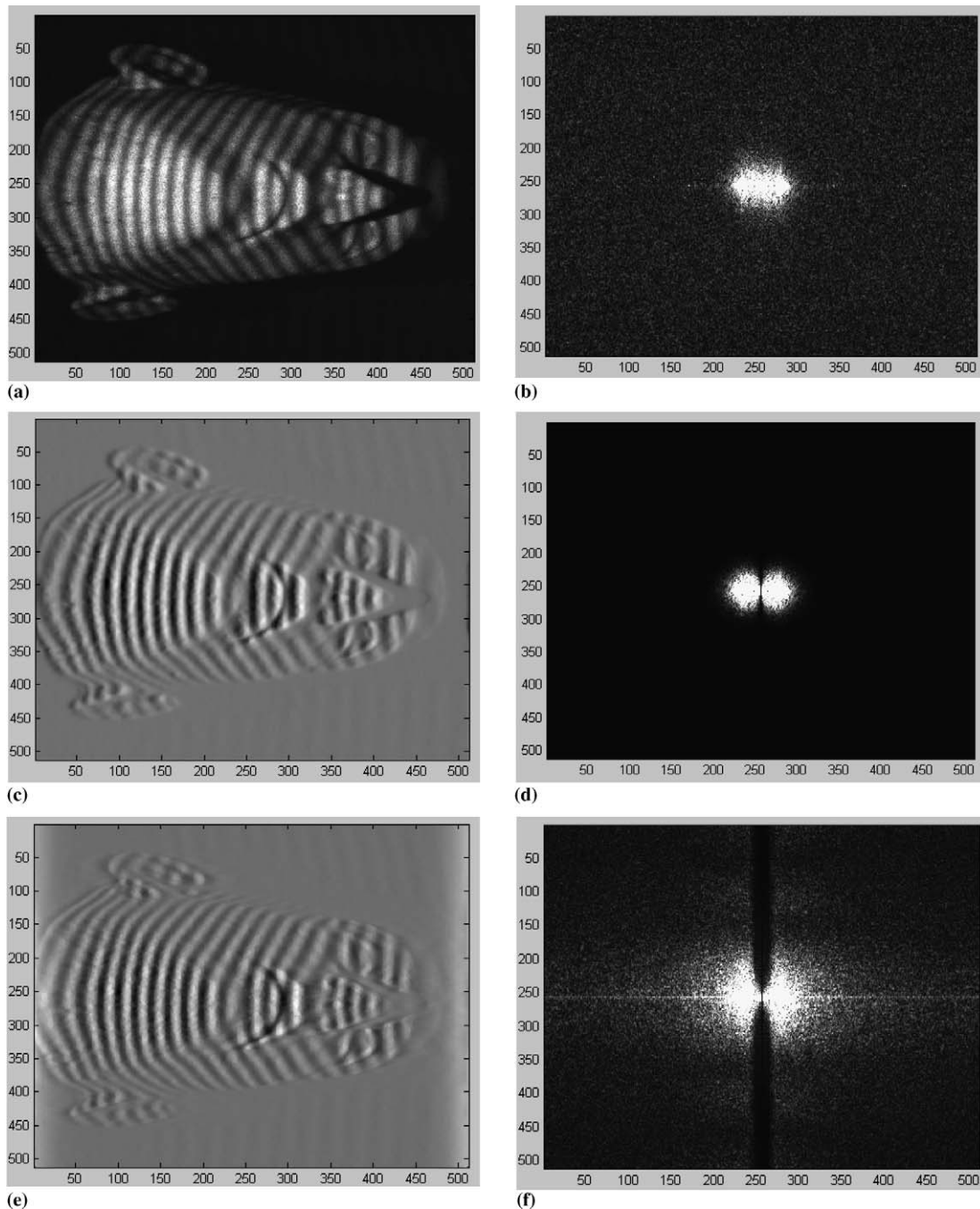


Fig. 5. (a) A non-full field fringe pattern, (c) and (e) the filtered fringe patterns using the 2D-CWT and Chen's algorithms, respectively. (b), (d) and (f) the spectrum of the fringe patterns shown in (a), (c) and (e), respectively.

5. Experimental results

The proposed algorithm has been tested using the real fringe pattern shown in Fig. 3(a). The fringe pattern can be considered as an interferogram with large bandwidth. Its contrast is very low. The detailed experiment setup to produce this fringe pattern is explained in Ref. [1]. The fringe pattern was filtered using the 2D-CWT method with scale 2 and angle 0. The resultant image is shown in Fig. 3(b). The proposed algorithm successfully removed the background illumination components from the fringe pattern. The algorithm also considerably reduced speckle noise, because the 2D-CWT behaves as a band-pass filter. The filtered fringe pattern was input to the FTP algorithm and the resultant wrapped phase is shown in Fig. 3(c). The wrapped phase was unwrapped using the algorithm in [18] and the resultant phase map is shown in Fig. 3(d).

The above experiment was repeated using Chen's algorithm. The window width was set to 64 and the moving factor is set to 3. Chen's algorithm wiped out the areas in the fringe pattern where the spatial frequency is high. The fringe pattern resulting from Chen's algorithm, shown in Fig. 3(e), was processed by the FTP algorithm and the resultant wrapped phase is shown in Fig. 3(f).

Row 100 of the real fringe pattern, filtered fringe patterns using 2D-CWT and Chen's algorithms are shown in Figs. 3(g)–(i), respectively. The visual inspection of the three figures indicates that the fringe pattern processed using Chen's algorithm has more distortion at its borders than the filtered fringe pattern using 2D-CWT algorithm.

Figs. 4(a)–(c) show the spectrum of the fringe pattern, the filtered fringe patterns using the 2D-CWT method and Chen's algorithm, respectively. Fig. 4(a) shows that there is interference in the frequency domain between the spectrum of the background illumination and the spectrum of the modulated fringes. The 2D-CWT algorithm was capable of filtering out the background illumination even with the existence of this interference, whereas Chen's algorithm failed to perform this task. This is illustrated in Figs. 4(b) and (c). The comparison between Figs. 4(b) and (c) revealed that the proposed 2D-CWT algorithm removed part of the high frequency noise from the fringe pattern.

The 2D-CWT has the ability to remove the background illumination of non-full field fringe patterns. Fig. 5(a) shows a non-full field fringe pattern for the Rando module explained in Ref. [1]. Also, the fringe pattern contains phase discontinuities and corrupted by speckle noise. The spectrum of the fringe pattern is shown in Fig. 5(b). The background illumination of the fringe pattern was filtered out using the 2D-CWT and Chen's algorithms and the resultant images are shown in Figs. 5(c) and (e), respectively. Figs. 5(d) and (f) depict the spectrum of the images shown in Figs. 5(c) and (e), respectively.

The visual inspection of Fig. 5 demonstrates that the proposed algorithm has better ability in removing the

background illumination and reduces the speckle noise of non-full field fringe patterns than Chen's algorithm.

The 2D-CWT algorithm was programmed in Matlab with the aid of the YAWTB toolbox [18]. The program was executed on a Pentium 4 computer with a 1.7 GHz clock speed and 1 GByte RAM memory. The execution time required to process a fringe pattern with 512×512 pixels on this hardware platform was approximately two seconds. Chen's algorithm was programmed using Matlab and the WaveLab toolbox [19]. Chen's algorithm required approximately 2 min to process the same fringe pattern on the same hardware platform.

6. Conclusions

The two-dimensional continuous wavelet transform has been used to eliminate the background illumination terms of a fringe pattern. The filtered fringe pattern has been subsequently processed using the Fourier transform profilometry algorithm. Experimental results demonstrate that the proposed algorithm is capable of removing the background illumination effectively, even when its spectrum interferes with the spectrum of the deformed fringes in the frequency domain. The algorithm also considerably reduces speckle noise in the fringe pattern. The proposed algorithm has been compared with Chen's algorithm and the experimental results demonstrate its superior performance.

References

- [1] F. Lilley, M. Lalor, D. Burton, *Opt. Eng.* 39 (2000) 187.
- [2] P. Hariharan, in: W.R. Robinson, G.T. Reid (Eds.), *Interferogram Analysis: Digital Fringe Pattern Measurement Techniques*, Institute of Physics, Philadelphia, PA, 1993.
- [3] M. Takeda, H. Ina, S. Kobayashi, *J. Opt. Soc. Am.* 72 (1982) 156.
- [4] K. Creath, in: W.R. Robinson, G.T. Reid (Eds.), *Interferogram Analysis: Digital Fringe Pattern Measurement Techniques*, Institute of Physics, Philadelphia, PA, 1993.
- [5] M. Gdeisat, D. Burton, M. Lalor, *Appl. Opt.* 39 (2000) 5326.
- [6] Y. Ichioka, M. Inuiya, *Appl. Opt.* 11 (1972) 1507.
- [7] D. Bone, H. Bachor, R. Sandeman, *Appl. Opt.* 25 (2000) 1653.
- [8] E.O. Brigham, *The Fast Fourier Transform and its Applications*, Prentice-Hall, New Jersey, 1988.
- [9] M. Takeda, K. Motoh, *Appl. Opt.* 22 (1983) 3977.
- [10] L. Jian, S. Xian-Yu, G. Lu-Rong, *Opt. Eng.* 29 (1990) 1439.
- [11] W. Chen, X. Su, Y. Cao, Q. Xiang, L. Xiang, *Opt. Las. Eng.* 43 (2005) 1267.
- [12] J. Antoine, R. Murenzi, P. Vandergheynst, S. Ali, *Two-Dimensional Wavelets and their Relatives*, Cambridge University Press, Cambridge, 2004.
- [13] D. Burton, M. Lalor, *SPIE* 1163 (1989) 149.
- [14] J. Antoine, D. Barache, R. Cesar, L. Fontoura Costa, *Signal Process.* 62 (1997) 265.
- [15] K. Kadooka, K. Kunoo, N. Uda, K. One, T. Nagayasu, *Exp. Mech.* 43 (2003) 45.
- [16] J.F. Kirby, *Comput. Geosci.* 31 (2005) 846.
- [17] M. Arevalillo Herraez, D. Burton, M. Lalor, M. Gdeisat, *Appl. Opt.* 41 (2002) 7437.
- [18] Yet another wavelet toolbox (YAWTB) home page. <http://www.fy-ma.ucl.ac.be/projects/yawtb/> (accessed 1.11.05).
- [19] WaveLab toolbox home page. www-stat.stanford.edu/~wavelab/ (accessed 1.11.05).